# NATIONAL ADVISORY COMMITTEE FOR AERONAUTICS

TECHNICAL NOTE

No. 1287

## FLIGHT TESTS OF AN AIRPLANE MODEL WITH A 42° SWEPT-BACK WING IN THE LANGLEY FREE-FLIGHT TUNNEL

By Bernard Maggin and Charles V. Bennett

Langley Memorial Aeronautical Laboratory
Langley Field, Va.

Washington
May 1947
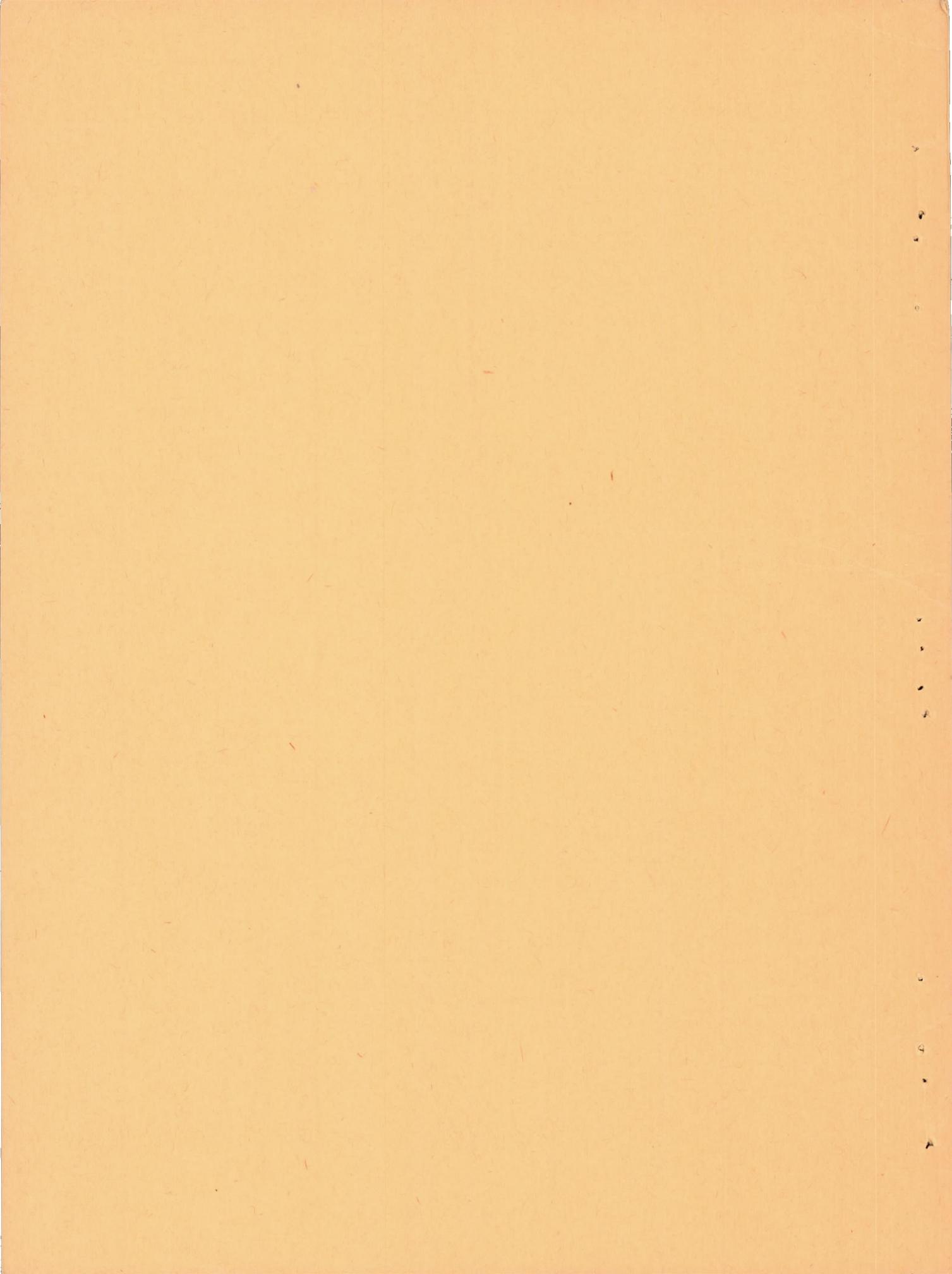
NATIONAL ADVISORY COMMITTEE FOR AERONAUTICS

TECHNICAL NOTE NO. 1287

FLIGHT TESTS OF AN AIRPLANE MODEL WITH A 42° SWEPT-BACK

WING IN THE LANGLEY FREE-FLIGHT TUNNEL

By Bernard Maggin and Charles V. Bennett

SUMMARY

Power-off flight tests have been conducted in the Langley free-flight tunnel to determine the dynamic stability characteristics of an airplane model with a 42° swept-back wing of aspect ratio 5.9 and taper ratio 0.5. The static-stability and wing-stall characteristics of the model were also determined.

The results of the investigation showed that although the wing alone was statically unstable longitudinally at moderate and high lift coefficients, the complete model was statically stable over the lift range for some horizontal-tail positions. The degree of stability, however, was critically dependent on tail position. The dynamic longitudinal stability noted in the flight tests was satisfactory except over a lift-coefficient range from 0.65 to 0.80 in which extreme difficulty was experienced in establishing the correct trim airspeed and flight-path angle. This difficulty, which has not been previously experienced in free-flight-tunnel investigations, was apparently associated with a change in air flow over the wing that caused abrupt changes in the variation of wing pitching moment and model flight-path angle with lift coefficient. The dynamic longitudinal behavior was erratic in this range of lift coefficient although the static longitudinal stability from force tests of the complete model appeared to be satisfactory. This particular phenomenon requires further investigation.

The lateral oscillation was predominantly a rolling motion, the damping of which was satisfactorily predicted by the lateral-stability theory that included product-of-inertia terms. When the product-of-inertia terms were neglected, the theory indicated instability for larger values of directional stability than observed in the flight tests.

The lateral control of the model was satisfactory at low lift coefficients. At high lift coefficients the lateral control was noticeably weaker but no great difficulty was encountered in maintaining

control up to the stall. At the stall the model dropped without
pitching or rolling off. The absence of rolling at the stall is
attributed to the fact that the swept wing maintains some damping
in roll at the stall in contrast to unswept wings which usually
autorotate at the stall.

## INTRODUCTION

A study is being made in the Langley free-flight tunnel of the
low-speed stability and control characteristics of airplane designs
having large amounts of sweepback. As a part of this study an
investigation has been made on a model with a $42^\circ$ swept-back wing of
aspect ratio 5.9 and taper ratio 0.5. This investigation included
power-off flight tests, force tests, tuft surveys, and damping-in-roll
tests of the model. The results of the damping-in-roll tests were
presented in reference 1 and all other results are presented herein.

The force tests were made with tails off and with various sizes
and positions of the vertical tail and various positions of the
horizontal tail. The flight tests were made over the lift range with
various amounts of directional stability. The tuft surveys were made
for the wing alone over the lift range. Calculations were made to
determine the boundary of zero damping of the lateral oscillations of
the model to obtain a correlation with the flight results.

## SYMBOLS

The forces and moments were measured about the stability axes.
A diagram of these axes showing positive directions of the forces and
moments is given in figure 1.

A        aspect ratio

S        wing area, square feet

V        airspeed, feet per second

W        weight of airplane, pounds

b        wing span, feet

$b_a$      aileron span, feet

| | |
|---|---|
| $c$ | wing chord, measured in plane parallel to plane of symmetry, feet |
| $c_a$ | aileron chord, feet |
| $\bar{c}$ | mean aerodynamic chord, measured in plane parallel to plane of symmetry, feet |
| $\Lambda$ | angle of sweepback of quarter-chord line of wing, degrees |
| $i$ | angle of incidence, degrees |
| $\alpha$ | angle of attack, degrees |
| $\lambda$ | taper ratio $(c_t/c_r)$ |
| $L$ | rolling moment, foot-pounds |
| $N$ | yawing moment, foot-pounds |
| $M$ | pitching moment, foot-pounds |
| $C_L$ | lift coefficient (Lift/qS) |
| $C_D$ | drag coefficient (Drag/qS) |
| $C_m$ | pitching-moment coefficient $(M/qS\bar{c})$ |
| $C_l$ | rolling-moment coefficient $(L/qSb)$ |
| $C_n$ | yawing-moment coefficient $(N/qSb)$ |
| $C_Y$ | lateral-force coefficient (Lateral force/qS) |
| $P$ | period of lateral oscillation, seconds |
| $q$ | dynamic pressure, pounds per square foot $\left(\frac{1}{2}\rho V^2\right)$ |
| $\rho$ | mass density of air, slugs per cubic foot |
| $\beta$ | angle of sideslip, degrees |
| $\mu$ | relative-density factor $(m/\rho Sb)$ |
| $m$ | mass, slugs |

$\dfrac{pb}{2V}$       helix angle generated by wing tip, radians

$p$       rolling angular velocity, radians per second

$r$       yawing angular velocity, radians per second

$\psi$       angle of yaw, degrees (for force-test data, $\psi = -\beta$)

$\phi$       angle of roll, degrees

$k_X$       radius of gyration about principal X-axis of inertia, feet

$k_Z$       radius of gyration about principal Z-axis of inertia, feet

$C_{l_\beta}$       effective-dihedral parameter, that is, rate of change of rolling-moment coefficient with angle of sideslip, per degree $\left( \partial C_l / \partial \beta \right)$

$\delta_a$       total aileron deflection, degrees (sum of deflections of right and left ailerons, equal up and down)

$C_{l_{\delta_a}}$       rolling-moment coefficient per degree deflection of one aileron $\left( \partial C_l / \partial \delta_a \right)$

$C_{n_\beta}$       directional-stability parameter, that is, rate of change of yawing-moment coefficient with angle of sideslip, per degree $\left( \partial C_n / \partial \beta \right)$

$C_{Y_\beta}$       lateral-force parameter, that is, rate of change of lateral-force coefficient with angle of sideslip, per degree $\left( \partial C_Y / \partial \beta \right)$

$C_{n_p}$       rate of change of yawing-moment coefficient with rolling-angular-velocity factor, per radian $\left( \partial C_n / \partial \dfrac{pb}{2V} \right)$

$C_{l_p}$       rate of change of rolling-moment coefficient with rolling-angular-velocity factor, per radian $\left( \partial C_l / \partial \dfrac{pb}{2V} \right)$

$C_{l_r}$       rate of change of rolling-moment coefficient with yawing-angular-velocity factor, per radian $\left( \partial C_l / \partial \dfrac{rb}{2V} \right)$

$C_{n_r}$    rate of change of yawing-moment coefficient with yawing-

angular-velocity factor, per radian $\left(\partial C_n / \partial \frac{rb}{2V}\right)$

R    Routh's discriminant

$\gamma$    flight-path angle, positive refers to climb, degrees

Subscripts:

t    tip

r    root

T    horizontal tail

## APPARATUS

The power-off flight and force tests were made in the Langley free-flight tunnel. The free-flight-tunnel balance rotates in yaw with the model so that all forces and moments are measured about the stability axes. (See fig. 1.) A complete description of the tunnel and balance is given in references 2 and 3, respectively. A photograph of the model in flight in the test section of the tunnel is shown in figure 2. Tuft tests of the model wing were made in the Langley 15-foot free-spinning tunnel.

A sketch of the model tested is shown in figure 3. The model consisted of a wooden boom upon which were mounted the wing and stabilizing surfaces. The wing had 42° sweepback of the quarter-chord line and a taper ratio of 0.5. The airfoil section perpendicular to the 0.50-chord line was a Rhode St. Genese 33 section. This section was used in accordance with free-flight-tunnel practice of using airfoil sections which obtain maximum lift coefficients in the low-scale tests approximately equal to that of a full-scale wing having conventional airfoil sections. The stabilizing surfaces were straight-taper unswept horizontal and vertical tails having NACA 0009 airfoil sections. Two vertical tails were tested on the model, one 10.6 percent of the wing area the other 5.25 percent of the wing area. The model was constructed so that the vertical- and horizontal-tail lengths could be varied and so that the vertical position of the horizontal tail could be adjusted. Figure 3 presents the geometric characteristics of the stabilizing surfaces and figure 4 presents the various positions of the surfaces for which tests were made.

## TESTS AND CALCULATIONS

Force tests were made to determine the lift, drag, and pitching-moment characteristics throughout the lift range for the model without the horizontal tail and with the horizontal tail in the three positions shown in figure 4. In addition, force tests were made at $\pm 5°$ yaw over the lift range to determine the lateral stability characteristics of the model with the vertical tail removed, with vertical tail 2 mounted in position 1, and with vertical tail 1 mounted in positions 1, 2, and 3. (See fig. 4.) For all these tests the horizontal tail was in position 1. All the force tests were made at a dynamic pressure of 3.0 pounds per square foot, which corresponds to a test Reynolds number of 271,000 based on the mean aerodynamic chord of 0.68 foot.

Tuft tests were made to study the flow pattern over the wing alone throughout the lift range. These tests were made at zero yaw at a dynamic pressure of 2.8 pounds per square foot, which corresponds to a test Reynolds number of 205,000. Photographs were taken of the upper surface of the wing over a range of angle of attack from $0°$ to $34°$.

Power-off flight tests of the model with the center of gravity at 0.55 mean aerodynamic chord were made throughout a lift-coefficient range from 0.48 to 1.02. In addition some flights were made with the center of gravity at 0.40 mean aerodynamic chord at a lift coefficient of approximately 0.75. For all these tests the vertical tail (tail 2) and the horizontal tail were mounted in position 1, respectively. Power-off flight tests were also made at a lift coefficient of approximately 0.6 with vertical tail 1 mounted in positions 1, 2, and 3. (See fig. 4.)

In the flights, abrupt deflections of approximately $\pm 18°$ (total $36°$) of the ailerons, $5°$ of the rudder, and $5°$ of the elevator were used for controlling the model. A complete description of the flight-testing technique used in the Langley free-flight tunnel is described in reference 2. The behavior of the model in flight under the various test conditions was noted by visual observations which were supplemented by motion-picture records.

Calculations were made by the method presented in reference 4 to determine the boundary of zero damping of the lateral oscillations of the model at lift coefficients of 0.8 and 0.4 to obtain a correlation with the flight results. Because a previous investigation (reference 5) showed that products of inertia in some conditions had a pronounced effect on lateral stability, two sets of calculations were made, one taking into consideration the product-of-inertia terms

and the other neglecting the product-of-inertia terms. For the
calculations in which the products of inertia were neglected, the
principal axes of inertia were assumed to coincide with the body
axes of the model. The aerodynamic, geometric, and mass charac-
teristics of the model used in the calculations are presented in
table I. The mass characteristics of the model were obtained by
measurements. The trim airspeed, flight-path angle, and angle of
attack for a lift coefficient of 0.8 were obtained from flight
tests. For a lift coefficient of 0.4 these values were obtained
from calculations and force tests. The values of $C_{Y_{\beta(tail\ off)}}$

and $C_{n_{\beta(tail\ off)}}$ were obtained from force tests and the values of

the damping-in-roll parameter $C_{l_p}$ were obtained from the experi-

mental data of reference 1. The values of the other stability
parameters were estimated from the charts of reference 6 with some
consideration being given to the effect of sweepback on these
parameters.

## RESULTS AND DISCUSSION

### Force Tests

Longitudinal stability.- The results of the force tests to
determine the lift, drag, and pitching-moment characteristics of the
model without a horizontal tail and with the horizontal tail in
position 1 are presented in figure 5. These data indicate that the
model with the horizontal tail off had unsatisfactory static longi-
tudinal stability characteristics at moderate and high coefficients
as evidenced by the increasing nosing-up moments as maximum lift is
approached. These data also indicate that with the horizontal tail
in position 1 the model had satisfactory static longitudinal stability
throughout the lift range. The downwash variation with lift coefficient
was extremely favorable in producing static longitudinal stability.
As the lift coefficient increased, the downwash apparently decreased
such that the horizontal tail became more effective. This increase
in effectiveness was great enough to straighten out the pitching-
moment curve for the complete model.

The results of the force tests made to determine the pitching-
moment characteristics of the model with various horizontal-tail
positions are presented in figure 6. These data are given with respect
to different center-of-gravity locations which give approximately equal
static margins over a moderate lift-coefficient range (0.2 to 0.6) so

that a direct comparison of the curves can be made. The data of
figure 6 show that moving the horizontal tail forward resulted
in a large decrease in static longitudinal stability at the
higher lift coefficients (0.7 to 1.1). Moving the horizontal tail
upward to a position that might be more suitable from high-speed-
flight considerations resulted in very marked instability over the
lift-coefficient range of 0.5 to 0.95. These data indicate that
severe changes in downwash exist behind the swept-back wing which
necessitates careful attention to horizontal-tail position in order
to obtain satisfactory static longitudinal stability characteristics
throughout the lift range.

Lateral stability.- The results of the force tests made to
determine the lateral stability characteristics of the model are
presented in figure 7 in the form of plots of the lateral-force
parameter $C_{Y_\beta}$, directional-stability parameter $C_{n_\beta}$, and
effective-dihedral parameter $C_{l_\beta}$ against angle of attack and
lift coefficient. These data show that with the vertical tail
removed, the model had a typical variation of $C_{l_\beta}$ with $C_L$ for
a swept-back wing. Adding the vertical tail reduced the variation
of $C_{l_\beta}$ with $C_L$ up to a $C_L$ of 0.7. This reduction results
because the vertical tail moves downward with increasing angle of
attack. The data of figure 7 also show that the model with vertical
tail removed had approximately zero directional stability $\left(C_{n_\beta} = 0\right)$
and that the addition of tail area and the increase in vertical-tail
length increased the directional stability as expected.

Flow Surveys

The results of the tuft tests of the wing alone are presented
in figure 8. These results are typical of moderate aspect-ratio wings
with fairly large amounts of sweepback. At low lift coefficients the
air flow over the wing is normal but at moderate lift coefficients
there is a spanwise air flow toward the wing tips along the trailing
edge of the wing. As the lift coefficient is increased, this outward
flow becomes more pronounced and effects chordwise stations
progressively farther ahead. At maximum lift coefficient all the flow
on the wing panels is outward and reverse flow and flow separation is
noted near the leading edge at the quarter span.

## Flight Tests

All the flight tests were made with the horizontal tail in position 1. This horizontal-tail position was chosen because force tests showed that with this tail position the most satisfactory static longitudinal stability was obtained throughout the lift range.

Longitudinal stability.- The dynamic longitudinal stability characteristics of the model with horizontal tail 1 and the center of gravity at 0.55 mean aerodynamic chord were considered satisfactory between lift coefficients of 0.48 to 0.65. In this lift-coefficient range the model flew steadily longitudinally and all pitching motions appeared to be heavily damped.

Over the lift-coefficient range from 0.65 to 0.80, satisfactory flights could not be obtained because of difficulty in establishing the correct trim airspeed and tunnel angle (which corresponds to the model flight-path angle). At times these settings would appear to be correct and the model would be flying satisfactorily but then suddenly, and for no apparent reason, the model would tend to rise or drop in the tunnel and large changes in tunnel angle and airspeed would be required to maintain flight. Often the changes required were so large that they could not be made quickly enough to prevent the model from crashing. This difficulty has never been experienced before in the Langley free-flight tunnel and must therefore be associated in some way with the particular swept-back wing tested ($\Lambda = 42^\circ$, $A = 5.9$, and $\lambda = 0.5$). The force tests indicate that the model has sufficient static longitudinal stability except possibly between lift coefficients of 0.65 and 0.75 (fig. 5). It was thought that the reduced stability between lift coefficients of 0.65 and 0.75 might explain the erratic flight behavior noted between lift coefficients of 0.65 and 0.80. A few flights made with the center of gravity moved forward 0.15 mean aerodynamic chord to increase the static longitudinal stability (fig. 9), however, did not result in an improvement in the longitudinal flight behavior in this lift coefficient range (0.65 to 0.80).

The erratic longitudinal flight behavior at lift coefficients between 0.65 and 0.80 might be the result of a change in air flow over the wing (indicated by the pitching-moment data of fig. 5 and tuft tests of fig. 8) combined with a large variation of the flight-path angle with lift coefficient (shown by the data of fig. 10). The erratic flight behavior of the model in the tunnel indicates that airplanes with wings which have abrupt changes in the variation of pitching moment with lift coefficient might have unsatisfactory dynamic longitudinal characteristics even though satisfactory static longitudinal stability is provided by a horizontal tail. This supposition is substantiated by figure 11 in which pitching-moment characteristics and flight-path angles for the model tested are compared with similar data for a model

having a wing with the same sweepback but a lower aspect ratio (3.0).
These data show that the low-aspect-ratio wing does not have as
abrupt a change in its pitching-moment curve as the high-aspect
ratio wing and has a smaller variation of flight-path angle with
lift coefficient.  The static longitudinal stability characteristics
of the complete models are similar and appear to be satisfactory.
In the flight tests with the model of aspect ratio 3.0, the dynamic
longitudinal stability was satisfactory at all lift coefficients
tested.  It appears therefore that the difficulties experienced in
flight with the model of aspect ratio 5.9 between lift coefficients
of 0.65 to 0.80 can be attributed to the abrupt changes in wing
pitching moment and flight-path angle.  The unsatisfactory longi-
tudinal stability noted in the model flights might be evidenced in
full-scale flight by difficulty in maintaining steady flight at lift
coefficients at which abrupt changes occur in the pitching-moment
characteristics of the wing.  This particular phenomenon requires
further investigation.

        In flights at lift coefficients between 0.80 and 1.02 with the
center of gravity at 0.55 mean aerodynamic chord, the longitudinal
stability was considered fairly satisfactory although not as good as
for lift coefficients between 0.48 and 0.65.  When the model reached
angles of attack that corresponded to the stall the model settled
to the tunnel floor without any pitching motion.

        Lateral stability and control.- With vertical tail 2 in position 1
the lateral stability characteristics of the model were considered
satisfactory throughout the lift-coefficient range investigated.  The
lateral motions, predominantly rolling accompanied by a small amount
of yawing, were fairly well damped.  Although aileron control was
noticeably weak at lift coefficients above 0.9, no great difficulty
was encountered in maintaining lateral control.  The ability to
maintain lateral control at high lift coefficients with reduced aileron
effectiveness is attributed to the fact that the wing damping in
roll $\left(C_{l_p}\right)$ at these high lift coefficients was also appreciably

reduced.  (See fig. 12.)

        At the stall no abrupt roll-offs occurred and the model usually
settled to the tunnel floor with wings level.  This good stalling
behavior is attributed to the slight positive damping in roll present
at the stall for this wing, which is in contrast to the negative
damping or autorotation at the stall for unswept wings.  (See fig. 12.)

        In the flights made with vertical tail 1 in positions 1, 2,
and 3 the reduction in tail size (tail 2 to tail 1) or the reduction
in tail length (positions 1 to 3) resulted in a progressive reduction
in the damping of the lateral oscillation.  Figure 13 presents the

results of motion-picture records of flights with controls fixed
made with vertical tail 1 in positions 1, 2, and 3. These data show
the reduced damping of the rolling motion as tail length was reduced
and indicate that with tail 1 in position 3 marginal lateral
stability was obtained.

The results of the calculations made to determine the boundary
of zero damping of the lateral oscillation (R = 0) are presented
and correlated with the flight results in figure 14. These data
show that the more complete theory, product-of-inertia terms included,
gives a satisfactory indication of the boundary for zero damping
of the lateral oscillation but that when product-of-inertia terms
are neglected the boundary for zero damping is not predicted with
satisfactory accuracy. When the product-of-inertia terms are
neglected, the boundary indicates lateral instability for larger
values of $C_{n_\beta}$ than those for which the flight tests indicated that
lateral instability exists. Neglecting the product-of-inertia terms
corresponds to the condition where the flight path and the principal
axes of inertia coincide, which could be accomplished on the model
by introducing the proper amount of wing incidence. A detailed
analysis of the effect of product of inertia on the lateral stability
boundary for zero damping of the lateral oscillation is given in
reference 5.

## CONCLUDING REMARKS

The results of force tests and power-off flight tests of an
airplane model with a 42° swept-back wing of aspect ratio 5.9 and
taper ratio 0.5 in the Langley free-flight tunnel are summarized
as follows:

1. Although the wing alone was statically unstable longi-
tudinally at moderate and high lift coefficients, the complete model
was statically stable over the lift range for some horizontal-tail
positions. The tests showed, however, that the static longitudinal
stability was critically dependent on tail position.

2. The dynamic longitudinal stability noted in the flight tests
was satisfactory except over a lift-coefficient range from 0.65
to 0.80 in which extreme difficulty was experienced in establishing
the correct trim airspeed and flight-path angle. This difficulty,
which has not been previously experienced in free-flight-tunnel
investigations, was apparently associated with a change in air flow
over the wing that caused abrupt changes in the variation of wing
pitching moment and model flight-path angle over this range of lift

coefficient.    The dynamic longitudinal behavior was erratic in this
lift-coefficient range although the static longitudinal stability
from force tests of the complete model appeared to be satisfactory.
This particular phenomenon requires further investigation.

3.    The lateral oscillation of the model was predominantly a
rolling motion which was well damped when a large vertical tail was
used.    Reducing the vertical-tail size or vertical-tail length
resulted in reductions in damping such that with the smallest tail
and the shortest tail-length configuration flown, the oscillation
was marginally stable.

4.    The boundary of zero damping of the lateral oscillation of
the model obtained in flight tests was predicted by the lateral-
stability theory that included product-of-inertia terms.    When the
product-of-inertia terms were neglected, the theory did not predict
the boundary for zero damping but indicated instability for larger
values of directional stability than observed in the flight tests.

5.    The lateral control of the model was satisfactory at low
lift coefficients.    At high lift coefficients the lateral control
was noticeably weaker but no great difficulty was encountered in
maintaining control.    This ability to maintain lateral control with
reduced aileron effectiveness was attributed to the reduced damping
in roll at these high lift coefficients.

6.    At the stall the model settled to the tunnel floor without
pitching or rolling off.    The absence of rolling is attributed to the
fact that the swept wing maintains some damping in roll at the stall
in contrast to an unswept wing which usually would autorotate at the
stall.

Langley Memorial Aeronautical Laboratory
     National Advisory Committee for Aeronautics
          Langley Field, Va., October 24, 1946

REFERENCES

1. Bennett, Charles V., and Johnson, Joseph L.: Experimental
   Determination of the Damping in Roll and Aileron Rolling
   Effectiveness of Three Wings Having 2°, 42°, and 62° Sweep-
   back. NACA TN No. 1278, 1947.

2. Shortal, Joseph A., and Osterhout, Clayton J.: Preliminary
   Stability and Control Tests in the NACA Free-Flight Wind
   Tunnel and Correlation with Full-Scale Flight Tests. NACA
   TN No. 810, 1941.

3. Shortal, Joseph A., and Draper, John W.: Free-Flight-Tunnel
   Investigation of the Effect of the Fuselage Length and the
   Aspect Ratio and Size of the Vertical Tail on Lateral
   Stability and Control. NACA ARR No. 3D17, 1943.

4. Zimmerman, Charles H.: An Analysis of Lateral Stability in
   Power-Off Flight with Charts for Use in Design. NACA Rep.
   No. 589, 1937.

5. Sternfield, Leonard: Effect of Product of Inertia on Require-
   ments for Lateral Stability. NACA TN No. 1193, 1947.

6. Pearson, Henry A., and Jones, Robert T.: Theoretical Sta-
   bility and Control Characteristics of Wings with Various
   Amounts of Taper and Twist. NACA Rep. No. 635, 1938.

TABLE I

CHARACTERISTICS OF AIRPLANE MODEL WITH 42° SWEPT-BACK WING USED

IN THE CALCULATIONS OF THE BOUNDARY OF ZERO DAMPING

OF THE LATERAL OSCILLATION  (R = 0)

|  | $C_L = 0.8$ | $C_L = 0.4$ |
|---|---|---|
| W/S, lb/sq ft | 1.85 | 1.85 |
| b, ft | 3.8 | 3.8 |
| $\rho$, slugs/cu ft | 0.00238 | 0.00238 |
| V, ft/sec | 44 | 62 |
| $\mu$ | 6.33 | 6.33 |
| $k_X$, ft | 0.51 | 0.51 |
| $k_Z$, ft | 1.29 | 1.29 |
| $C_{l_p}$, per radian | 0.17 | -0.28 |
| $C_{l_r}$, per radian | $0.142 - 0.099C_{n_{\beta(tail)}}$ | $0.108 + 0.060C_{n_{\beta(tail)}}$ |
| $C_{n_p}$, per radian | $-0.0406 - 0.099C_{n_{\beta(tail)}}$ | $-0.0309 - 0.060C_{n_{\beta(tail)}}$ |
| $C_{n_r}$, per radian | $-0.0131 - 1.2C_{n_{\beta(tail)}}$ | $-0.0071 - 1.2C_{n_{\beta(tail)}}$ |
| $C_{Y_\beta}$, per radian | $-0.0074 - 1.67C_{n_{\beta(tail)}}$ | $-0.0074 - 1.67C_{n_{\beta(tail)}}$ |
| $C_{n_{\beta(tail\ off)}}$, per radian | 0 | 0 |
| $\gamma$, deg | -9 | -10 |
| $\alpha$, deg | 10 | 2 |

Fig. 1                                            NACA TN No. 1287
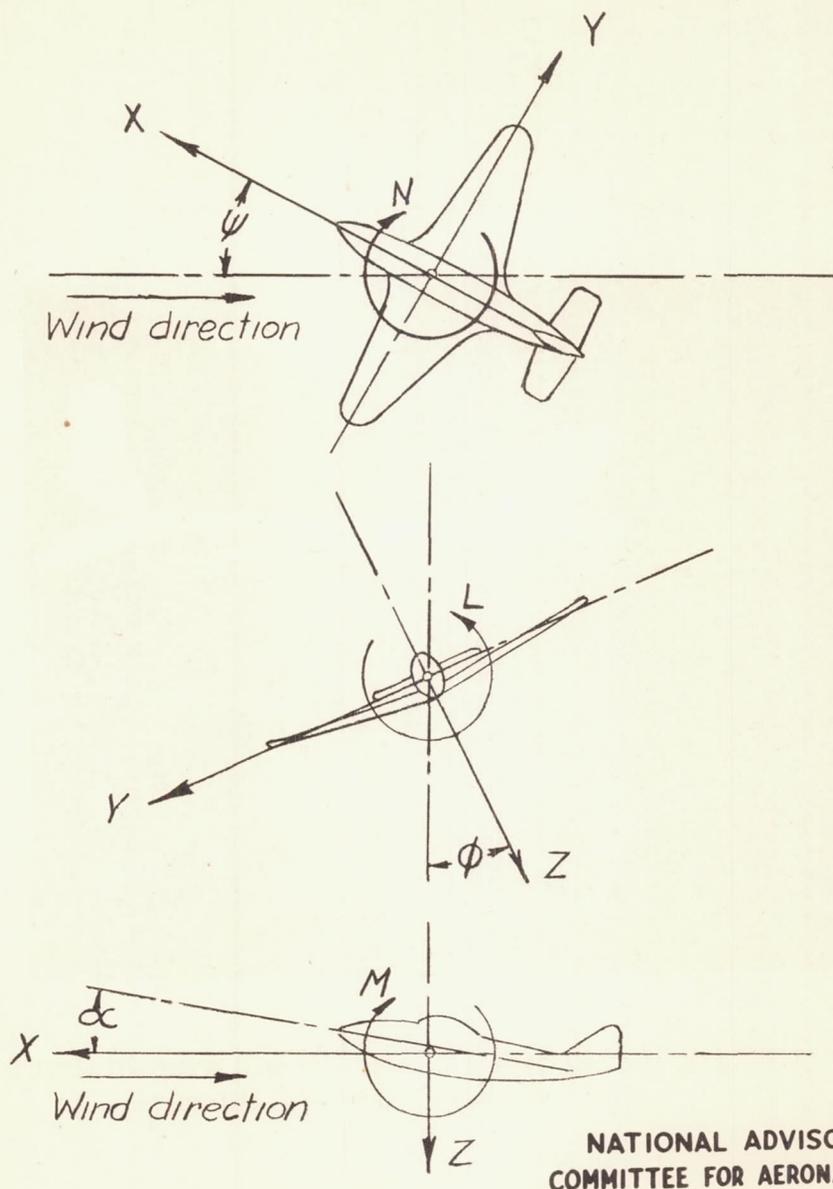


Figure 1.— The stability system of axes. Arrows indicate
  positive directions of moments and forces. This
  system of axes is defined as an orthogonal system
  having its origin at the center of gravity and in
  which the Z-axis is in the plane of symmetry and
  perpendicular to the relative wind, the X-axis is in
  the plane of symmetry and perpendicular to the
  Z-axis, and the Y-axis is perpendicular to the
  plane of symmetry.
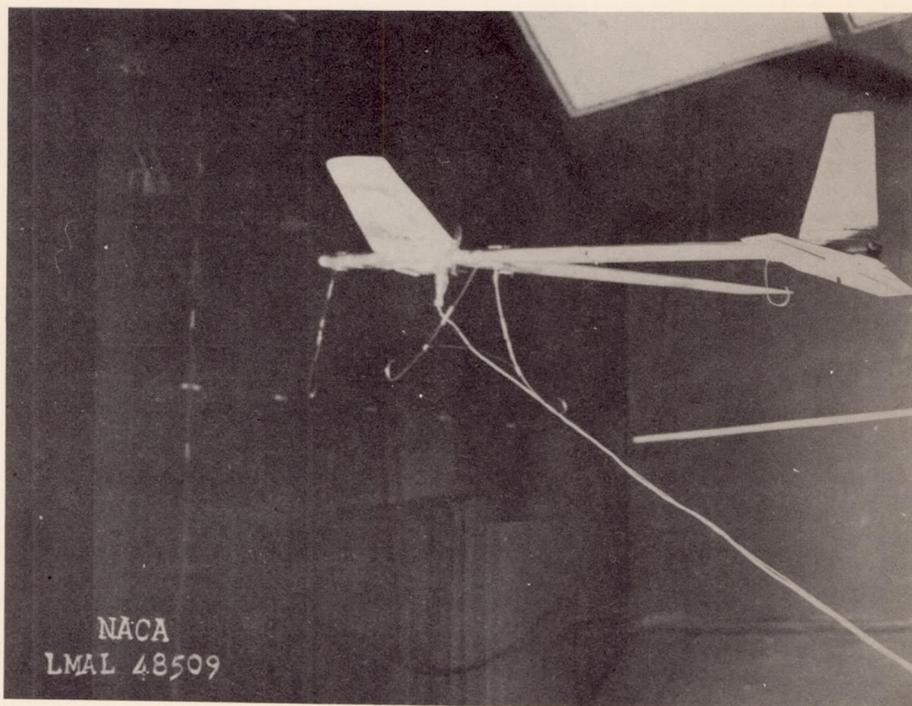
Figure 2.-   Airplane model with 42° swept-back wing in flight in
the Langley free-flight tunnel.

Figure 3.— Airplane model with 42° swept-back wing tested in the Langley free-flight tunnel. Wing airfoil section, Rhode St. Genese 33, perpendicular to 0.50-chord line; tail airfoil sections, NACA 0009.

Fig. 4

NACA TN No. 1287

Vertical-tail position  3     2      1

.67b

.44b

.24b

Rudder
hinge line

Tail 1

c.g. at .55 c̄

Vertical-tail positions tested

Horizontal-tail position  2  1  3

c.g. at .55 c̄

Tail 2

10"

Elevator
hinge line

2.5 c̄

3.8 c̄

$i_t = -5°$

Horizontal-tail positions tested

**NATIONAL ADVISORY
COMMITTEE FOR AERONAUTICS**

Figure 4.- Vertical- and horizontal-tail
positions tested in free-flight-
tunnel investigation of an airplane
model with 42° swept-back wing.
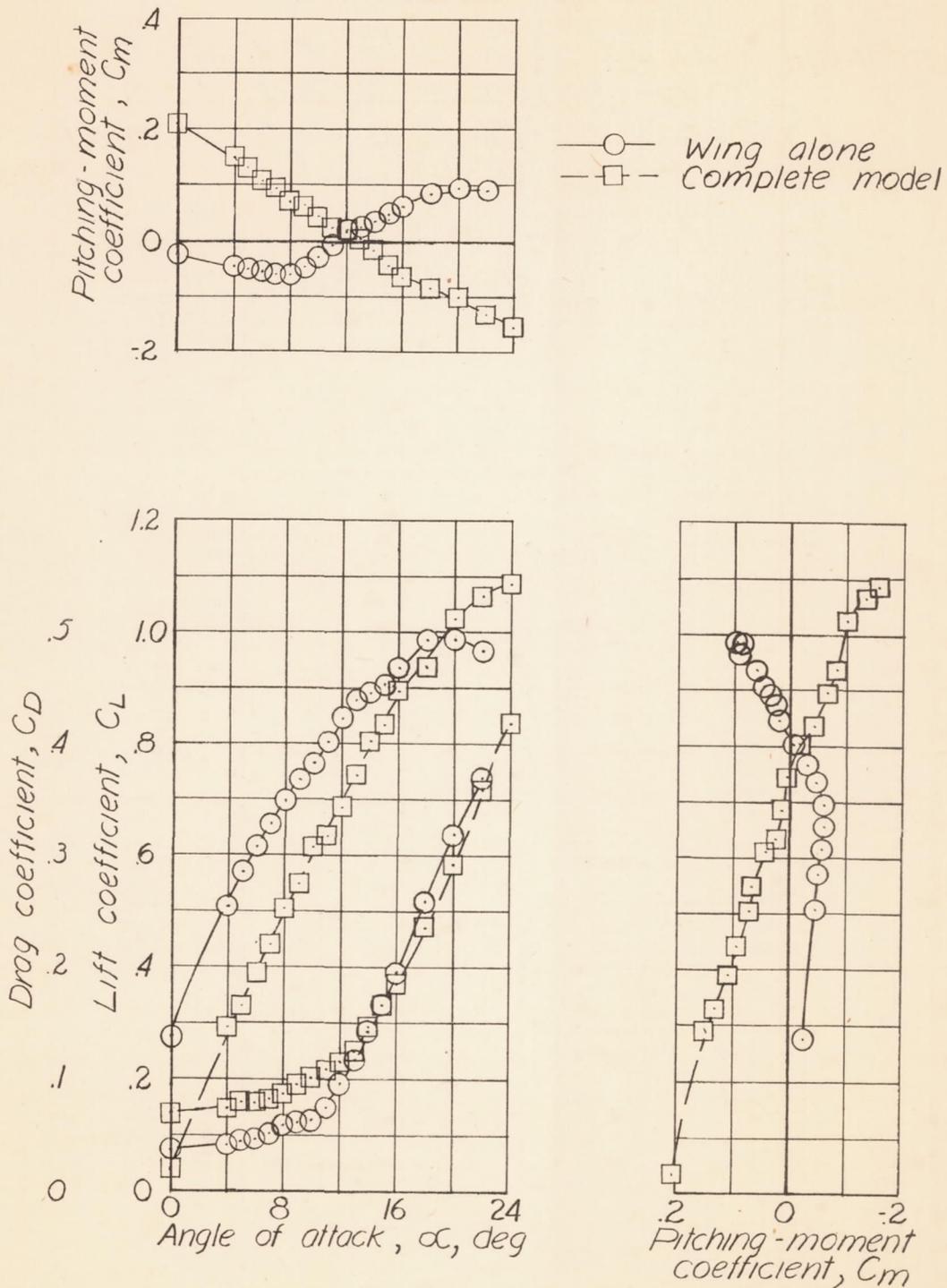
Figure 5.- Variation of the static longitudinal force characteristics of the airplane model with 42° swept-back wing. Vertical tail 2 in position 1; horizontal tail in position 1; center of gravity at 0.55 c̄.

Fig. 6                                              NACA TN No. 1287

| | Horizontal-tail position | c.g. (percent c̄) |
|---|---|---|
| ─○─ | 3 | 53 |
| ─□─ | 2 | 45 |
| ─◇─ | 1 | 55 |

Horizontal-tail position

1

2

3

Lift coefficient, $C_L$

NATIONAL ADVISORY
COMMITTEE FOR AERONAUTICS

Pitching-moment coefficient, $C_m$
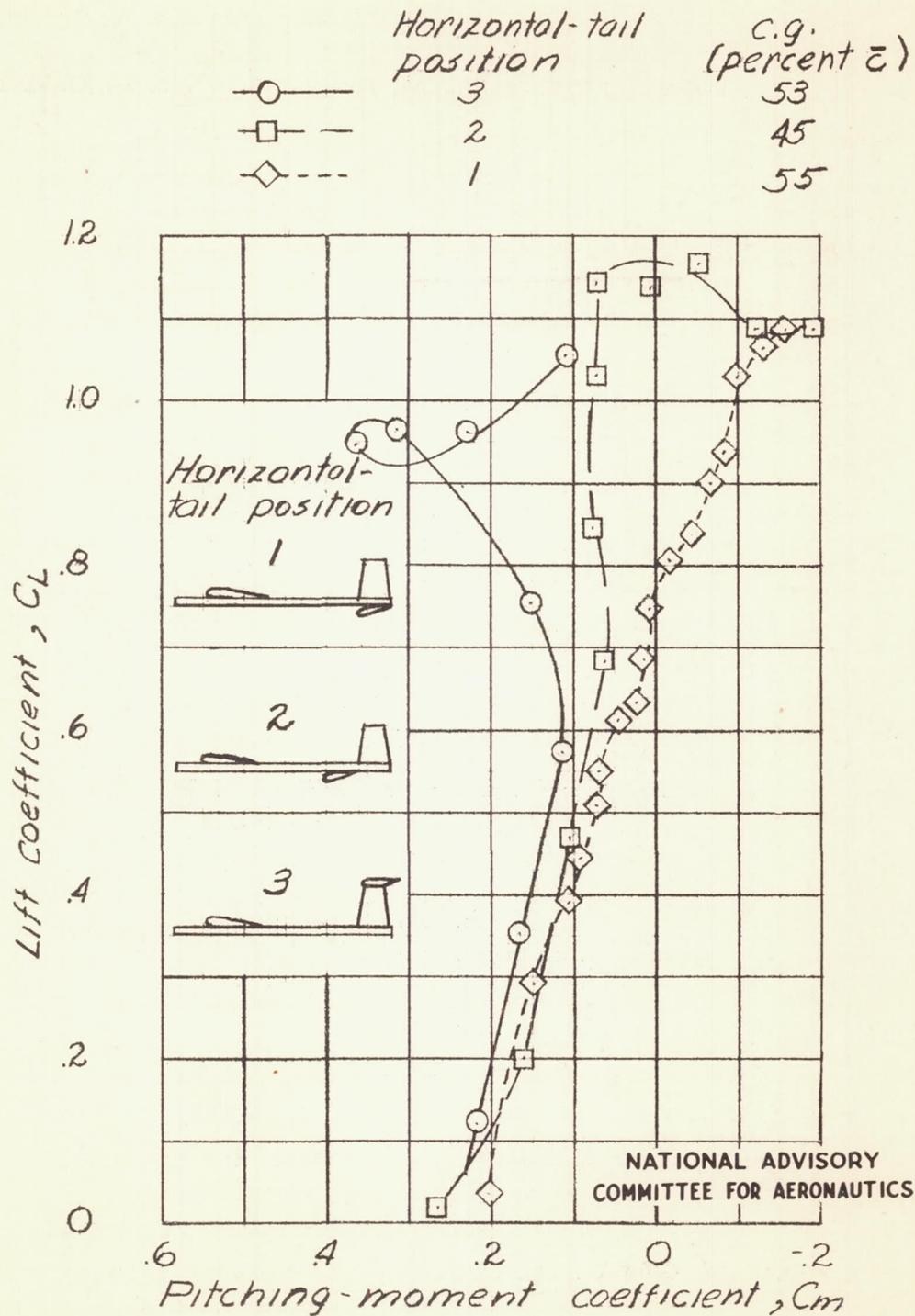
Figure 6.- Effect of horizontal-tail position
on the pitching-moment characteristics
of the airplane model with a 42° swept-
back wing. Vertical tail 2 in position 1.

Fig. 7

Tail | Tail position
○ | 1 | 1
□ | 2 | 1
◇ | off | 2
△ | 1 | 3
▽ | 1 |

Lateral-force parameter, $C_{Y_\beta}$

0

.02

Directional-stability parameter, $C_{n_\beta}$

.004

.002

0

-.002

Effective-dihedral parameter, $-C_{l_\beta}$

-.004

-.002

0

.002

Lift coefficient, $C_L$

0    .4    .8    1.2

Angle of attack, $\alpha$, deg

0    8    16    24    32

Lift coefficient, $C_L$

0    .4    .8    1.2

Angle of attack, $\alpha$, deg

0    8    16    24    32
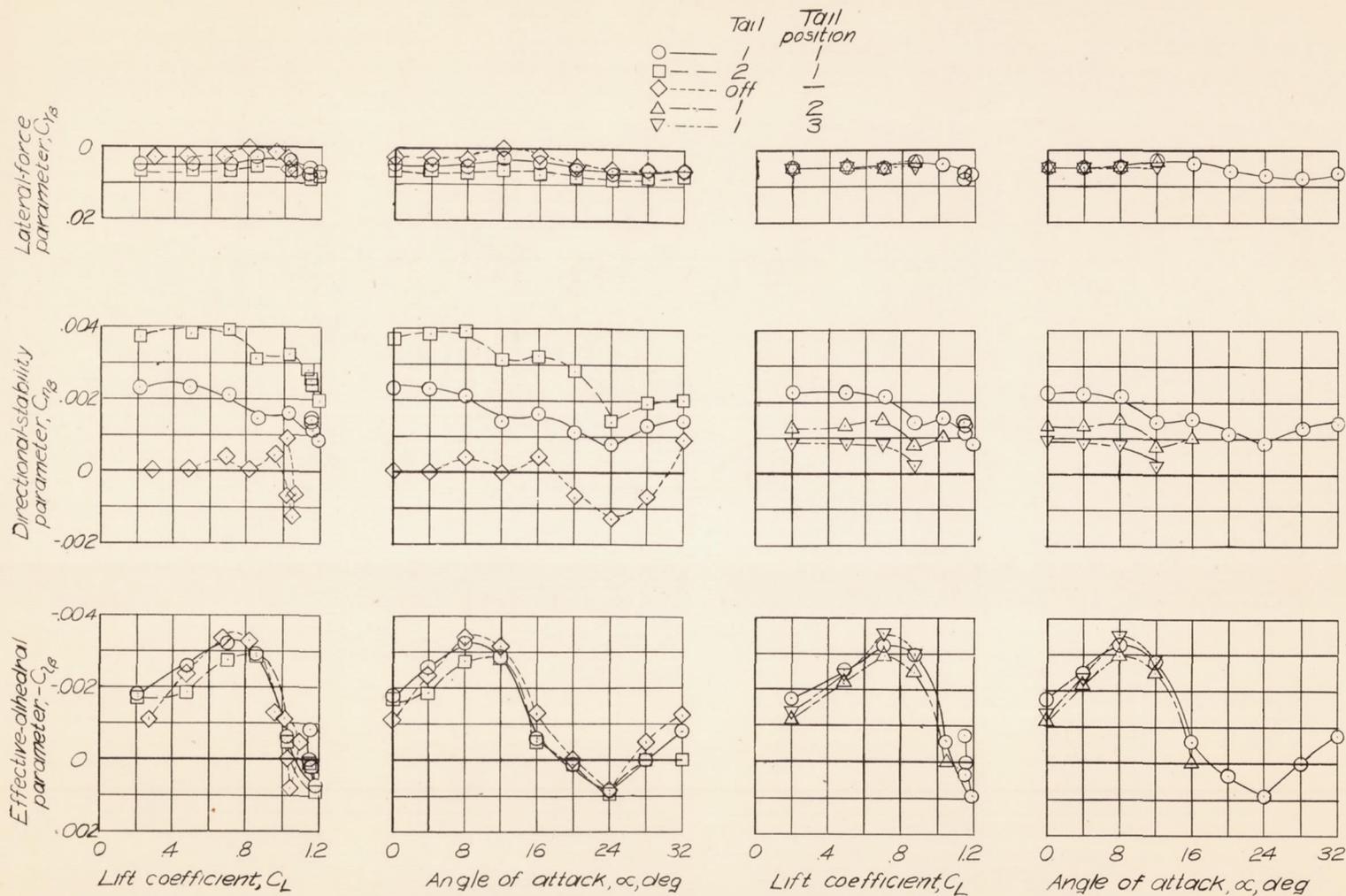
NATIONAL ADVISORY
COMMITTEE FOR AERONAUTICS

Figure 7. – Variation of the lateral-stability parameters $C_{Y_\beta}$, $C_{n_\beta}$, and $C_{l_\beta}$ with $C_L$ and $\alpha$ for the airplane model with 42° sweptback wing with various vertical-tail arrangements.
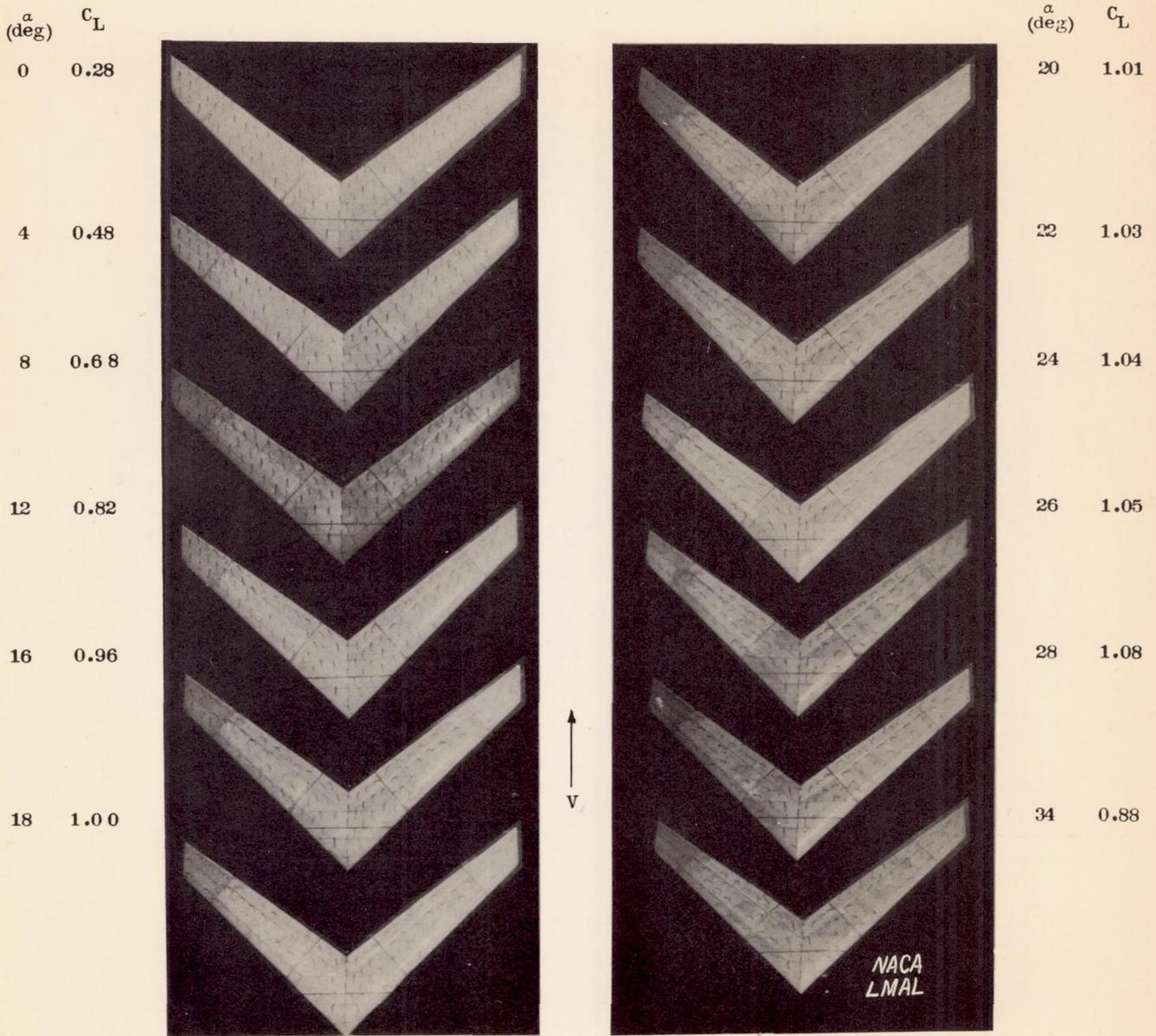
Figure 8.-   Tuft tests of swept-back wing used in flight tests.
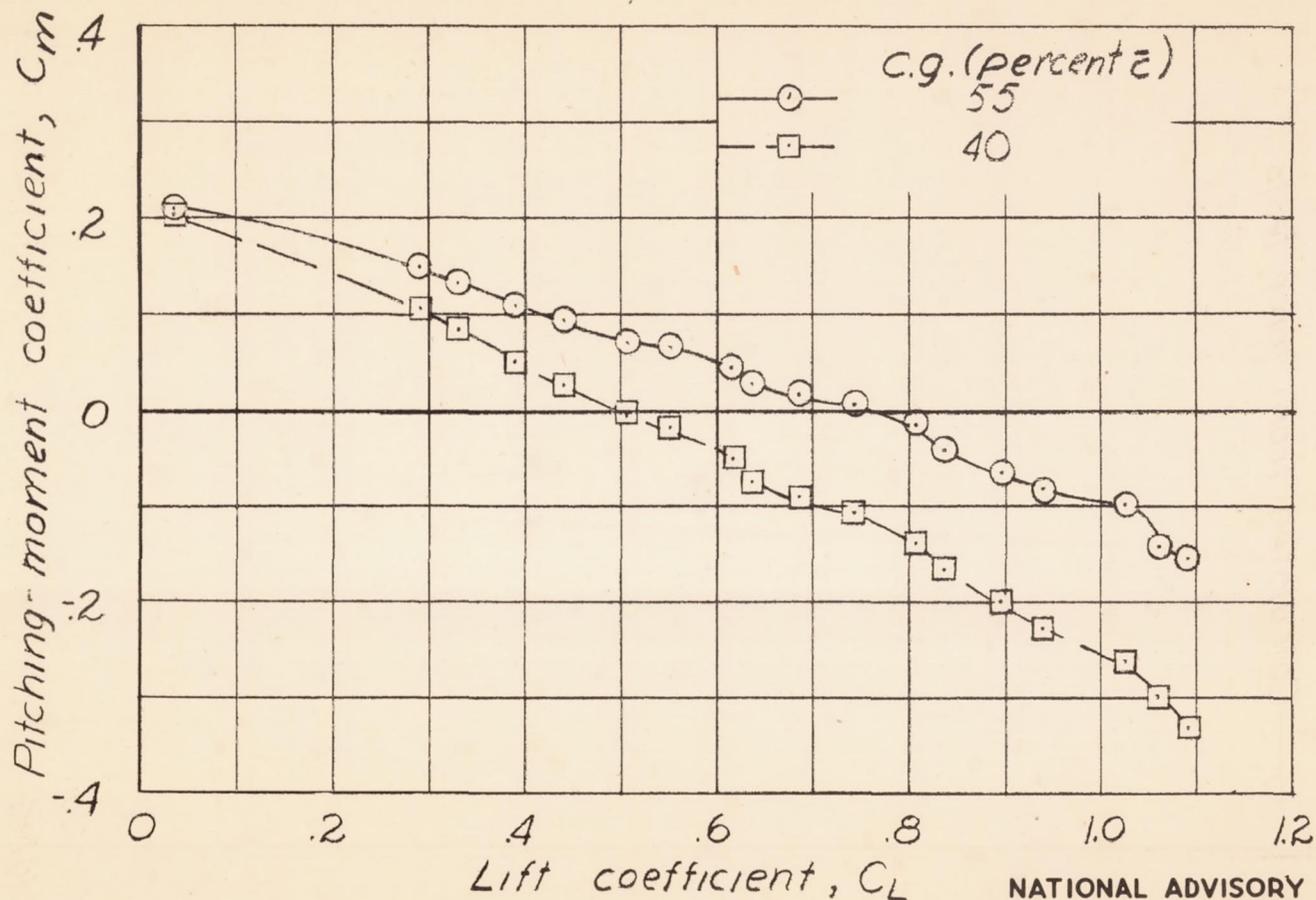
Figure 9. — Effect of 0.15 shift in center of gravity on the static longitudinal stability characteristics of airplane model with a 42° swept-back wing.

Fig. 9

Fig. 10                                    NACA TN No. 1287
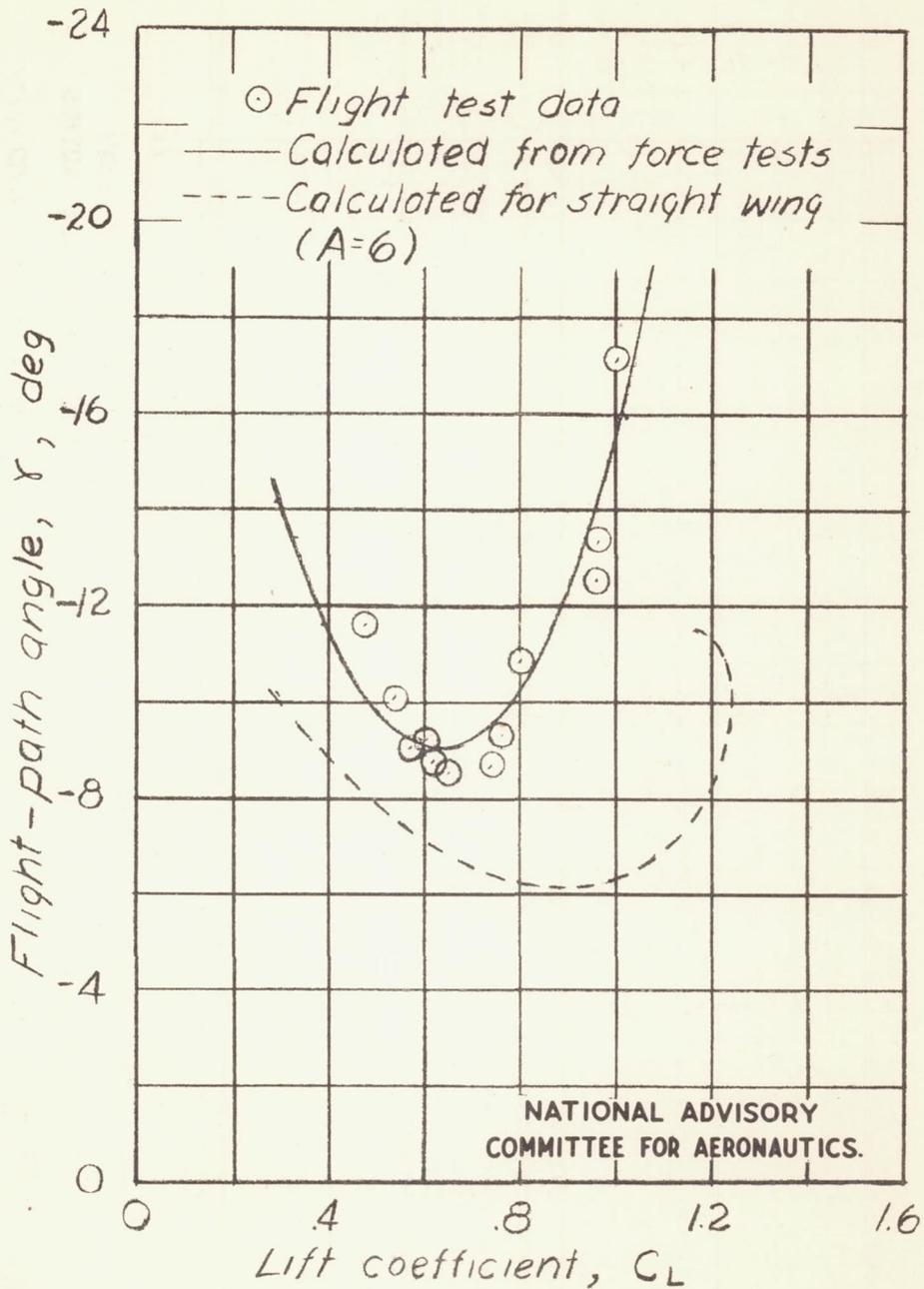


Figure 10.- Comparison of experimental and calculated values of flight-path angles required for the model tested with a 42° swept-back wing and those calculated for a similar model with a straight wing.

| Configuration | A | λ | c.g. (percent c̄) |
|---|---|---|---|
| Wing alone | 5.9 | 0.5 | 25 |
| Wing alone | 3.0 | 0.707 | 25 |
| Complete model | 5.9 | 0.5 | 45 |
| Complete model | 3.0 | 0.707 | 85 |
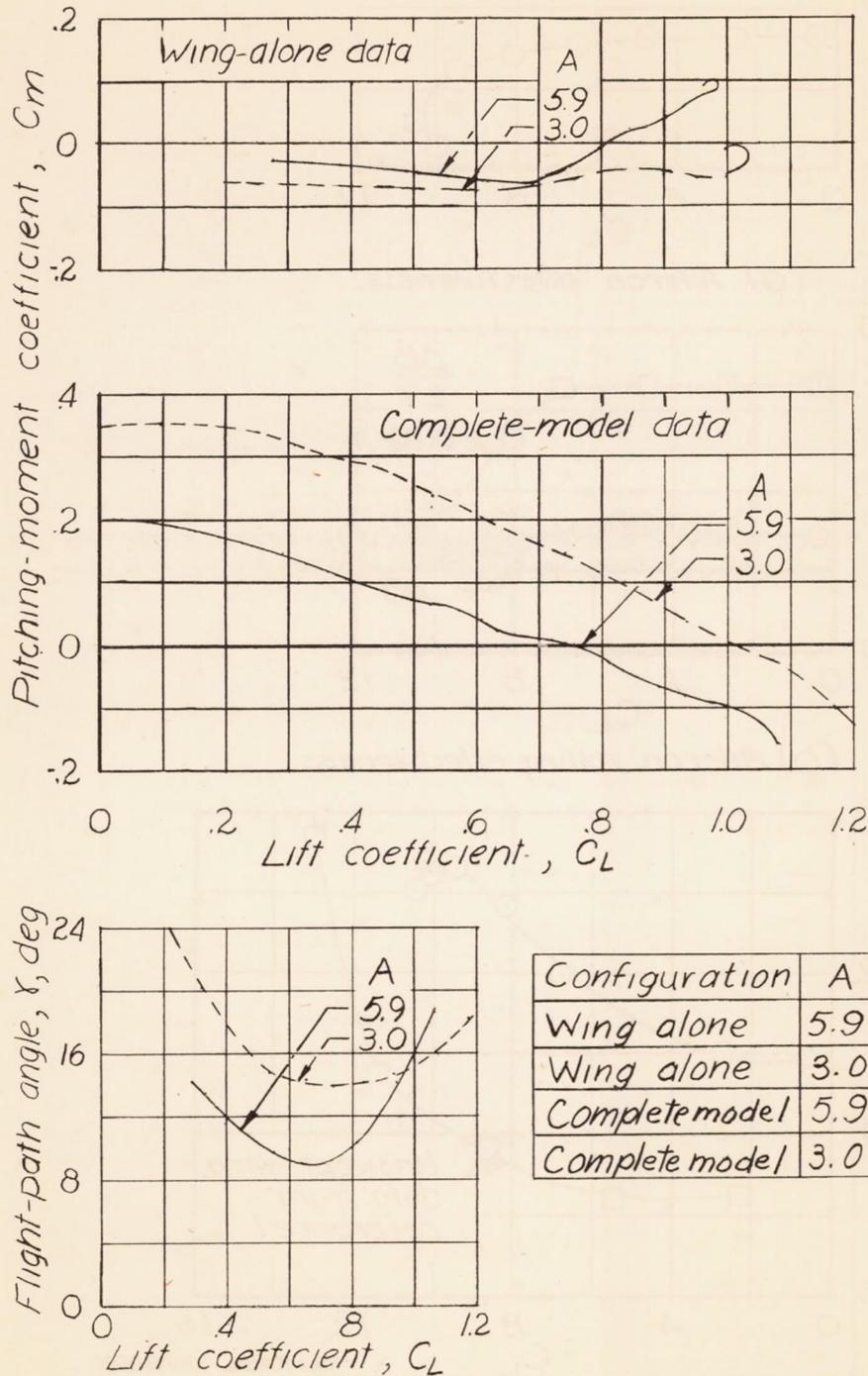
NATIONAL ADVISORY
COMMITTEE FOR AERONAUTICS

Figure 11.- Comparison of the pitching-moment characteristics and flight-path angles of two airplane models with 42° swept-back wings and aspect ratios of 5.9 and 3.0.

Fig. 12                                                    NACA TN No. 1287
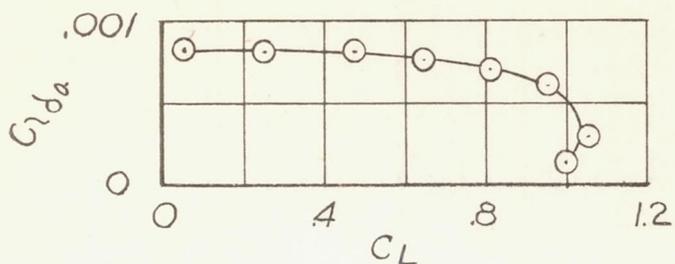


(a) Aileron effectiveness.
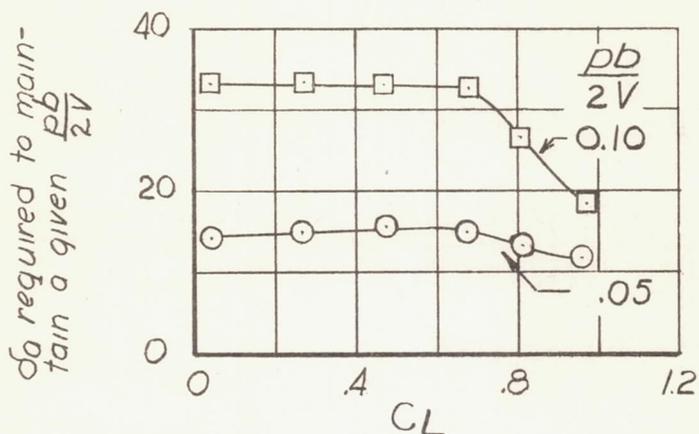
(b) Aileron rolling effectiveness.
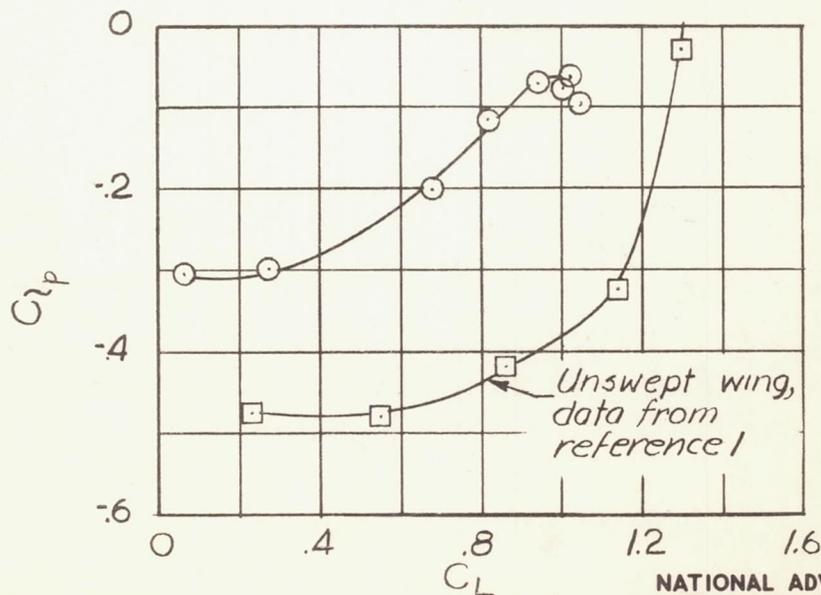
(c) Damping in roll.

NATIONAL ADVISORY
COMMITTEE FOR AERONAUTICS

Figure 12.- Variation of $C_{l_p}$, $C_{l_{\delta_a}}$, and $\delta_a$ required for rolling with $C_L$ for a 42° swept-back wing. $A=5.9$; $\lambda=0.5$; $c_a=0.30c$; $b_a=0.50b$. Data from reference 4.

$C_{n_\beta} = 0.0022$    $P = 1.2$

$C_{l_\beta} = -0.0030$    $C_L = 0.62$

Tail position 1

$C_{n_\beta} = 0.0013$    $P = 1.25$

$C_{l_\beta} = -0.0030$    $C_L = 0.62$

Tail position 2

$C_{n_\beta} = 0.0008$    $P = 1.25$

$C_{l_\beta} = -0.0030$    $C_L = 0.60$
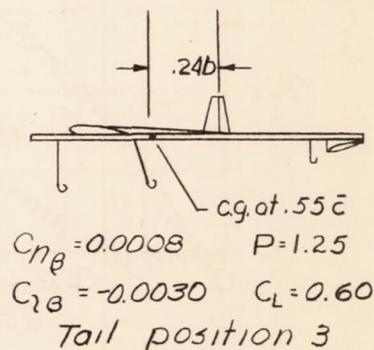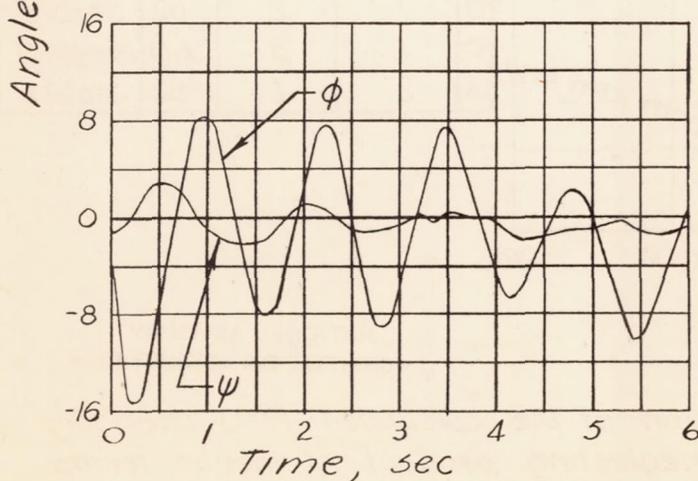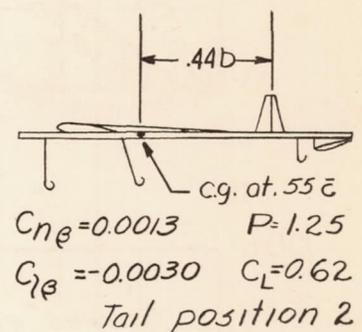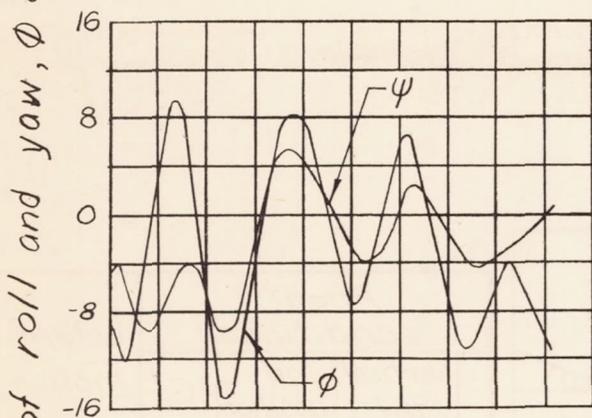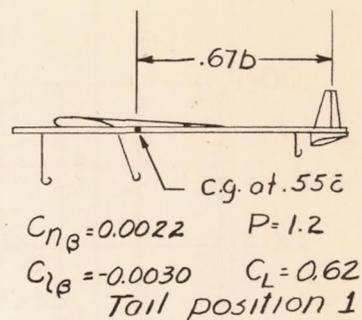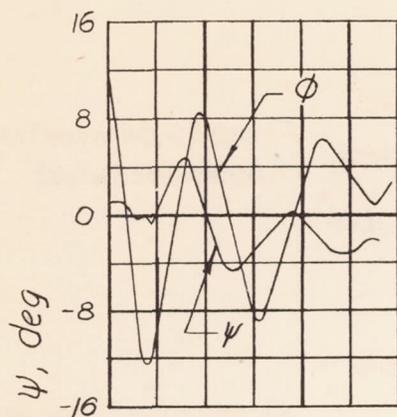
Tail position 3

NATIONAL ADVISORY
COMMITTEE FOR AERONAUTICS

Figure 13.- The variation of roll angle $\phi$ and yaw angle $\psi$ with time for the airplane model with a 42° swept-back wing in flight. Vertical tail 1 in positions 1, 2, and 3. Data obtained from motion-picture records. Controls fixed.
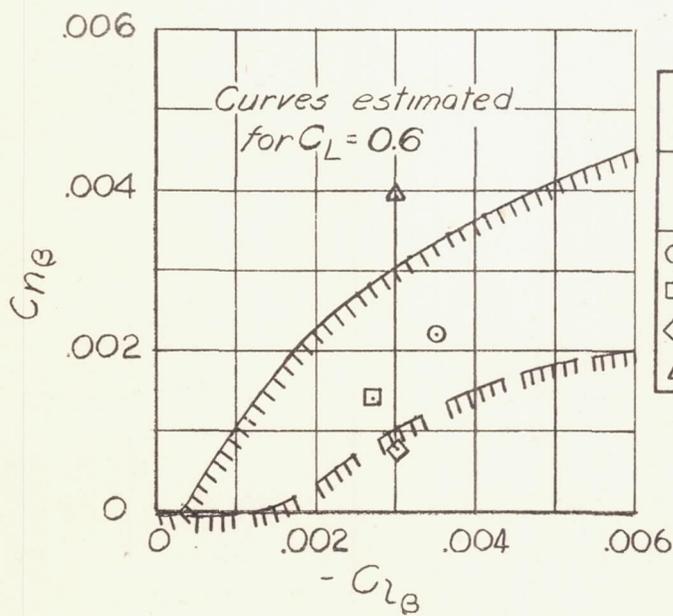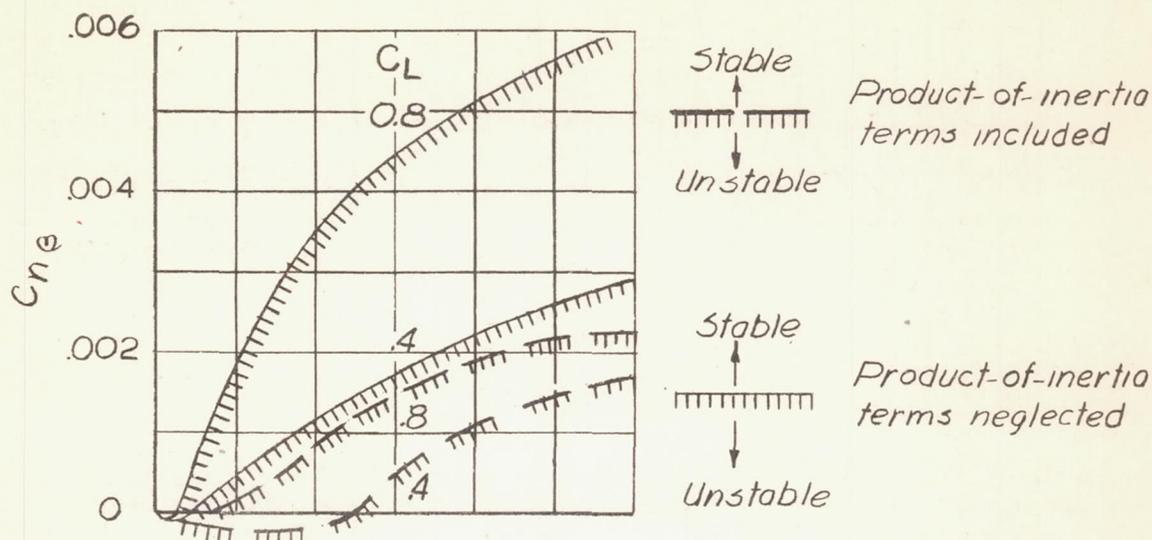
Fig. 14                                                            NACA TN No. 1287



Figure 14.- Correlation of the calculated R=0 boundary including and neglecting product-of-inertia terms with flight-test results.